PhD Study at Cardiff School of Mathematics

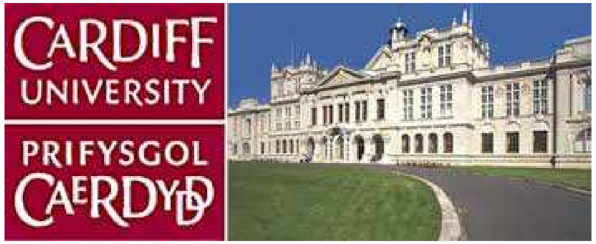

Cardiff University, Wales, UK

PROGRAMME OF STUDY

Supervised research project leading to thesis (3-3.5 years full time)

Postgraduate lecture courses (100 credits):
MAGIC (Mathematics Access Grid Instruction and Collaboration) - 20 UK Universities;
NATCOR (National Taught Course Center in Operational Research) - 13 UK Universities.

Annual progress review conducted by a panel consisting of project supervisor
and two other faculty members

Final viva voce examination conducted by one internal and one external examiner

Graduation

RESEARCH ENVIRONMENT

Individual Workplace and Computing Facilities

Participation in Scientific Meetings (seminars, national and international conferences), including the Annual Welsh Mathematics Colloquium at Gregynog Hall

SIAM (Society for Industrial and Applied Mathematics) Student Chapter

Postgraduate Seminar Programme (organised by students)

Cardiff University Graduate College Training Courses

APPLICATION PROCESS

Appropriate Undergraduate Degree (1 or 2:1 class) or Master Degree Required

Academic Supervisor for Research Project Available

Funding Obtained (EPSRC/Cardiff University Scholarship, Supervisor's Research Grant, Other sources)

On-Line Application via Cardiff University Website:
http://www.cardiff.ac.uk/maths/degreeprogrammes/postgraduate/research/application/

Entry dates: 1 October, 1 January, 1 April, 1 June

Biogenic Load-Bearing Structures

Modelling, Analysis, Computations

L Angela Mihai

(Cardiff University)

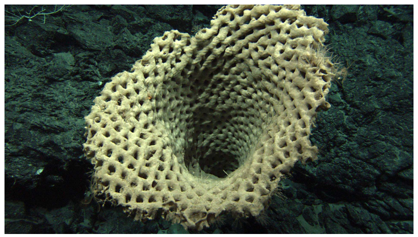
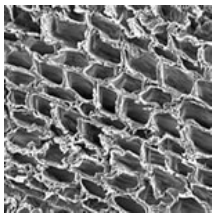


Historical Background

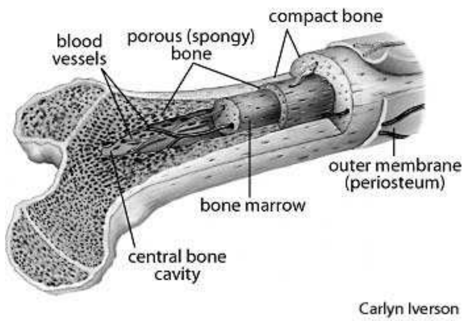

Robert Hooke (1635-1703) ◇ introduced the word 'cell' to describe the microscopic structure of cork ◇ as well as the famous law: 'as the force, so the extension'.

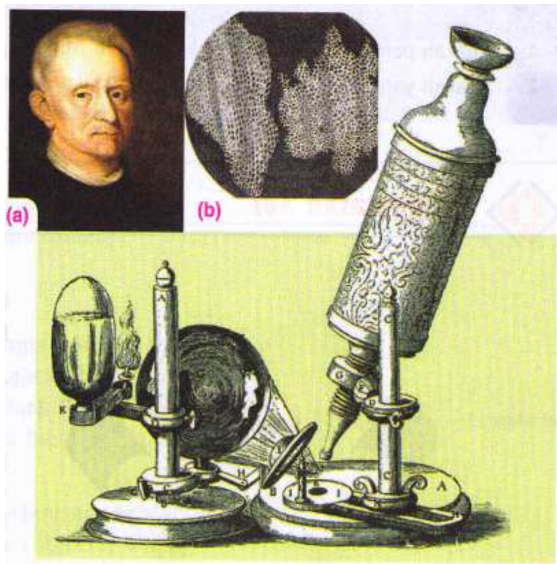

Galileo Galilei (1564-1642) ◇ bones must be hollow to afford maximum strength to weight ratio ◇ bones of larger animals must be thicker in proportion to their size than those of smaller animals.

Soft Wood

(a) (b)

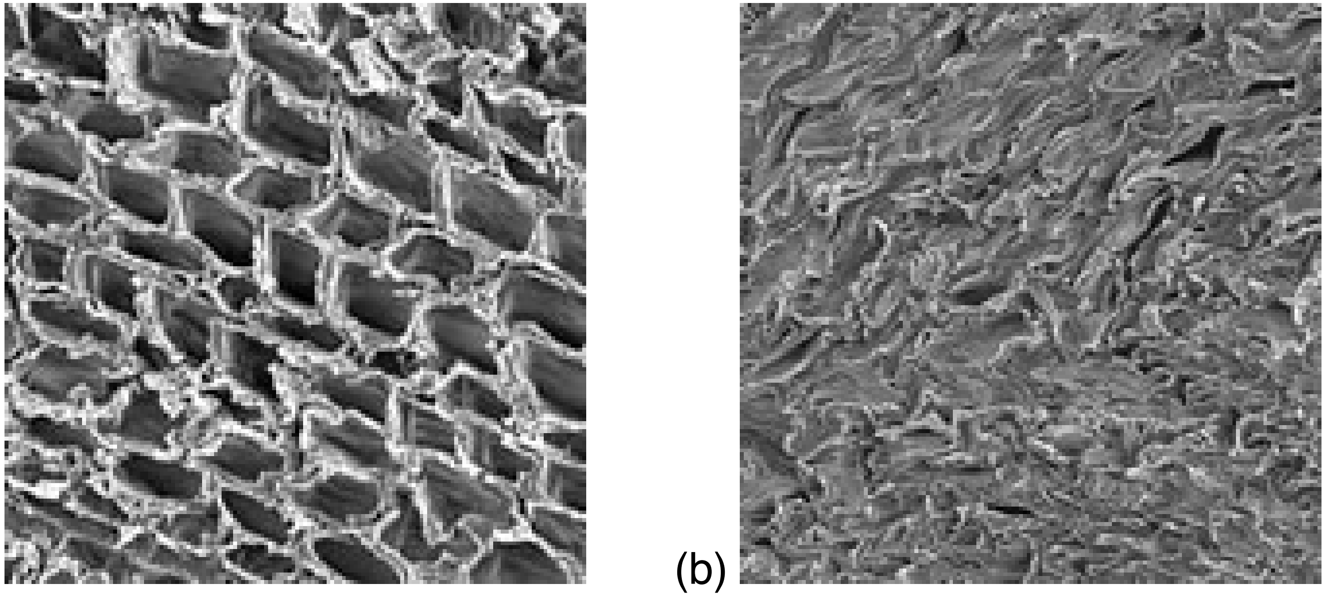

Japanese cedar wood (a) before and (b) after densification at Hida Sangyo (one of the most historic woodwork furniture manufacturers in Japan).

Paws and Plantar Pads

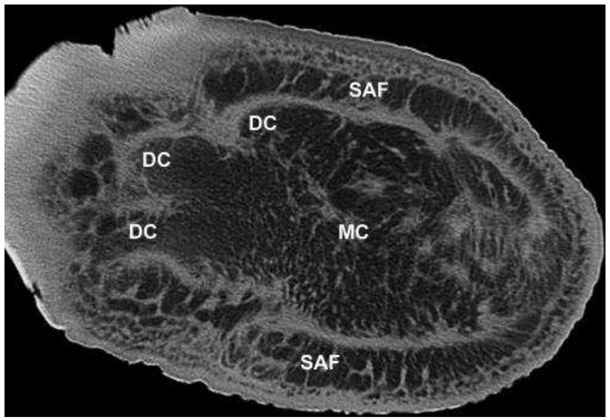

Biogenic Cellular Structures

The following main factors determine the magnitude of stress level in biogenic cellular structures [Scanlon 2005]:

◇ Poisson's ratio ◇ Cell wall thickness ◇ Cell inclusions

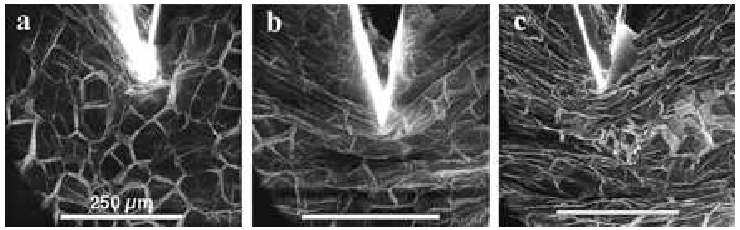

Large deformation near the tip of a knife slicing a carrot: (a) fresh carrot, (b) one-week-old carrot, (c) three-week-old carrot [Thiel & Donald 1998].

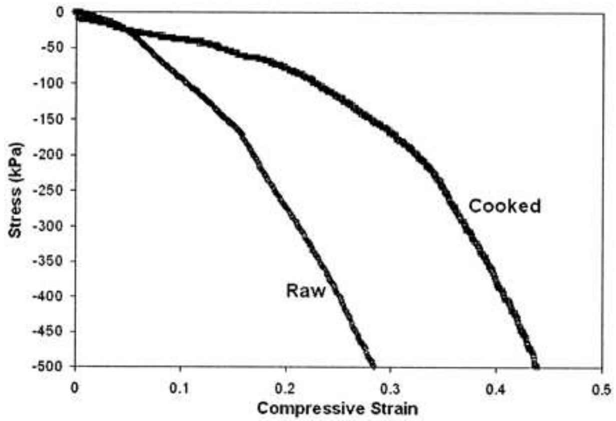

Stress-strain curves collected during in situ compression of carrot specimens [Warner et al. 2000].

Mathematical Modelling of Cellular Solid Materials

◇ At low stresses or strains, the mechanism which dominates the deformation of cellular solids is that of bending of the cell walls (e.g. metal foams) [Gibson & Ashby 1997].

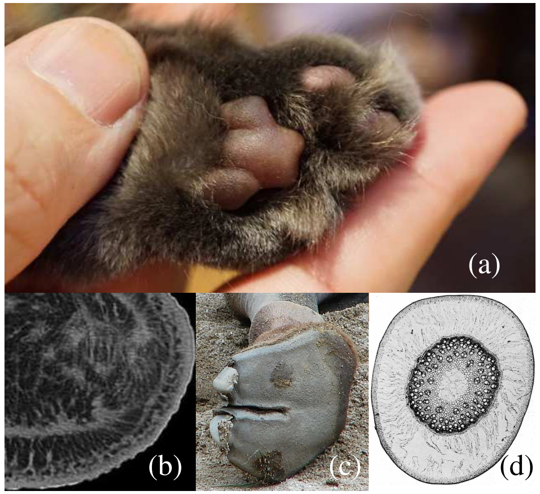

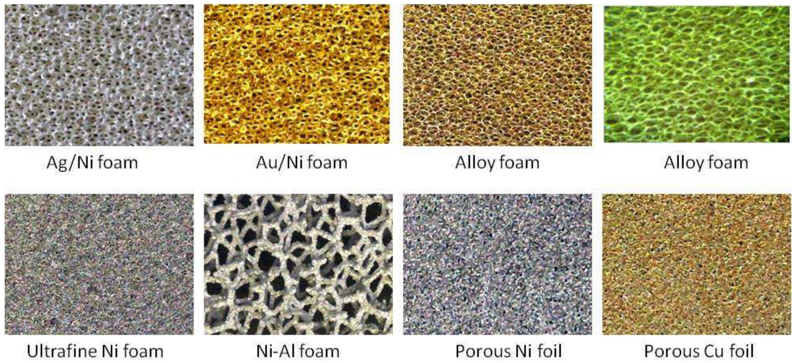

◇ At large strains, the deformation of cellular bodies is inherently nonlinear, and the corresponding stresses depend on both the position and the underlying material properties [AM & Goriely 2014, 2015].

Finite Elastic Deformations

Changes of length, area, and volume in the deformation $x = \chi(X)$ are governed by the deformation gradient $F = \nabla\chi$, such that $J = \det F > 0$.

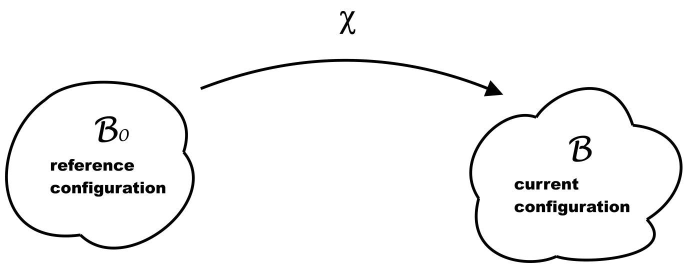

Various nonlinear strain measures:

- Left Cauchy-Green strain $B = FF^T$;
- Right Cauchy-Green strain $C = F^T F$;
- Green-Lagrange strain $E = (C - I)/2$;
- Logarithmic strain $\ln C^{1/2}$.

For a homogeneous, isotropic, incompressible hyperelastic material characterised by the strain energy density $\mathcal{W}(X, F)$, the internal force per unit of deformed area acting within the deformed solid is given by the Cauchy (true) stress tensor:

$$\boldsymbol{\sigma} = -pI + \beta_1 B + \beta_{-1} B^{-1}, \quad -p \text{ (hydrostatic pressure)}, \; \beta_1 > 0, \; \beta_{-1} \leq 0$$

Bending of a Pre-Stressed Elastic Cell Wall

T1. For a cell wall $(X, Y, Z) \in [C_1, C_2] \times [-Y_0, Y_0] \times [-Z_0, Z_0]$ bent into a sector of a circular cylindrical tube (annular wedge) by the deformation:

$$r = \sqrt{2AaX}, \quad \theta = \frac{BY}{\sqrt{a}}, \quad z = \frac{Z}{AB\sqrt{a}}$$

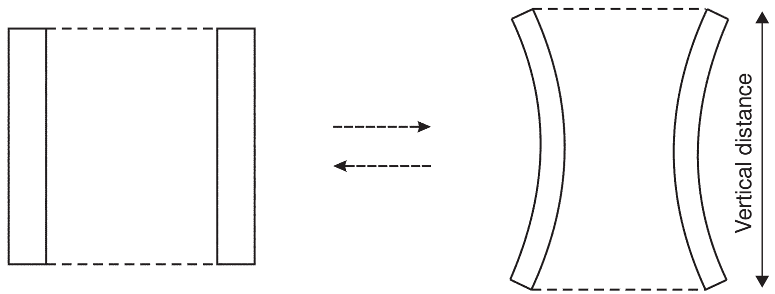

- The radial elastic modulus is greater in the closed cell filled with an incompressible fluid than in the open cell, and the gap between the moduli increases as cell pressure increases:

$$\frac{\bar{\sigma}_{rr}}{\ln \bar{C}_{rr}^{1/2}} - \frac{\sigma_{rr}}{\ln C_{rr}^{1/2}} > -\frac{p_0}{\ln C_{rr}^{1/2}} \geq 0.$$

- This elastic modulus increases when the thickness of the cell wall increases:

$$\frac{\sigma'_{rr}}{\ln C'^{1/2}_{rr}} - \frac{\sigma_{rr}}{\ln C_{rr}^{1/2}} > 0.$$

Straightening of a Pre-Stressed Annular Wedge

T2. When an annular wedge $(R,\Theta,Z)\in[R_1,R_2]\times[-\Theta_0,\Theta_0]\times[-Z_0,Z_0]$ is 'straighten' into a rectangular block by the deformation:

$$x=\frac{AB^2a}{2}R^2,\quad y=\frac{\Theta}{AB},\quad z=\frac{Z}{Ba}$$

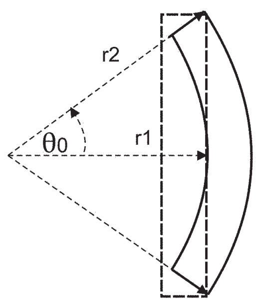

Open cell

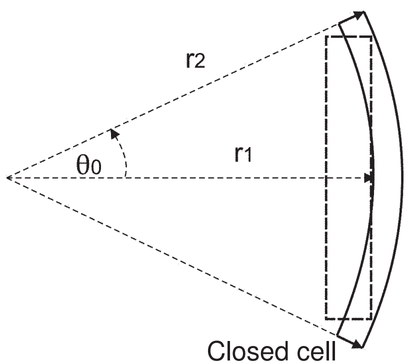

Closed cell

- The elastic modulus in the first and second direction is greater in the closed cell filled with an incompressible fluid than in the open cell, and the gap between the moduli increases as cell pressure increases:

$$\frac{\bar{\sigma}_{xx}}{\ln \bar{C}_{xx}^{1/2}}-\frac{\sigma_{xx}}{\ln C_{xx}^{1/2}}=-\frac{p_0}{\ln C_{xx}^{1/2}}\geq 0,$$
$$\frac{\bar{\sigma}_{yy}}{\ln \bar{C}_{yy}^{1/2}}-\frac{\sigma_{yy}}{\ln C_{yy}^{1/2}}>-\frac{p_0}{\ln C_{yy}^{1/2}}\geq 0.$$

- Since $\sigma_{xx}/\ln C_{xx}^{1/2}$ and $\sigma_{yy}/\ln C_{yy}^{1/2}$ increase as x increases, these elastic moduli increase when the thickness of the cell wall increases.

Stretching and Twisting of a Pre-Stressed Circular Tube

T3. When a circular tube $(R, \Theta, Z) \in [R_1, R_2] \times [-\Theta_0, \Theta_0] \times [-Z_0, Z_0]$ is subjected to the combined stretch and torsion:

$$r = \sqrt{AaR^2 + B}, \quad \theta = \Theta + \frac{\tau Z}{a}, \quad z = \frac{Z}{Aa}$$

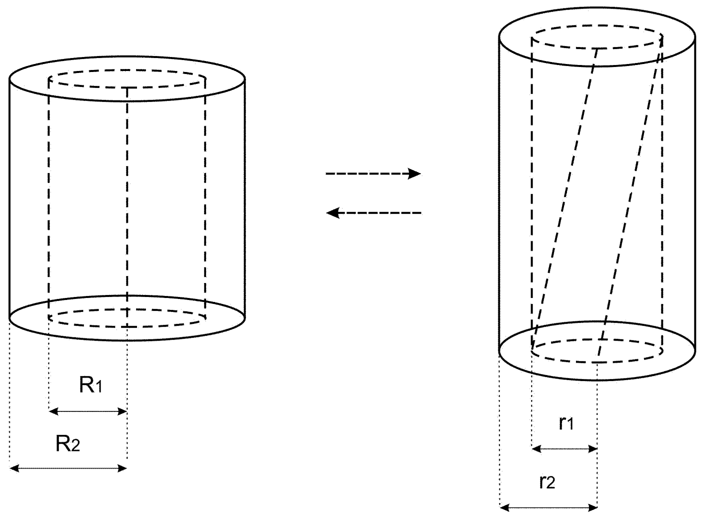

- The radial elastic modulus is greater in the closed tube filled with an incompressible fluid than in the open tube, and the gap between the moduli increases as cell pressure increases:

$$\frac{\bar{\sigma}_{rr}}{\ln \bar{C}_{rr}^{1/2}} - \frac{\sigma_{rr}}{\ln C_{rr}^{1/2}} = -\frac{p_0}{\ln C_{rr}^{1/2}} \geq 0.$$

- This elastic modulus increases when the thickness of the tube wall increases:

$$\frac{\sigma'_{rr}}{\ln C'^{1/2}_{rr}} - \frac{\sigma_{rr}}{\ln C_{rr}^{1/2}} > 0.$$

Honeycombs and Cellular Pads in Vertical Tension or Compression

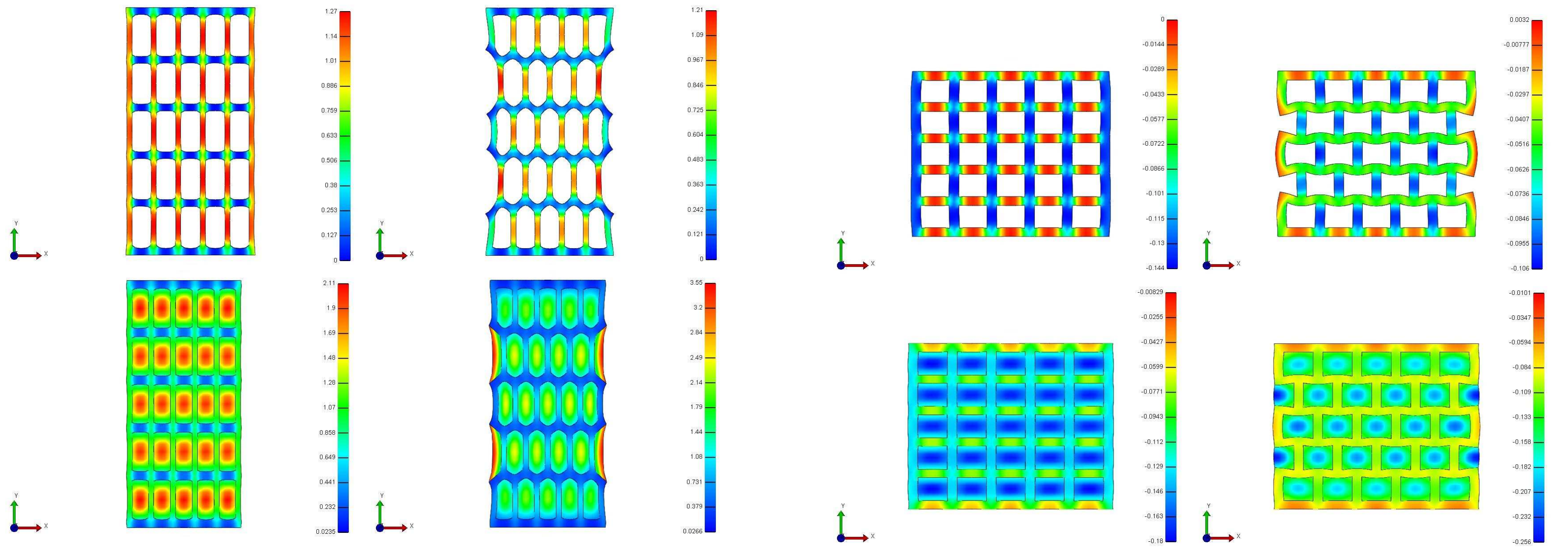

Vertical component of the Green-Lagrange (engineering) strain tensor $E_{22} = (C_{22} - 1)/2$ under prescribed vertical displacement of 0.75 (left) and -0.14 (right) at the top boundary [FEBio 2012].

Mechanical Behaviour in Vertical Tension

◇ The apparent elastic modulus of cell walls $E_L = \sigma_{22} / \ln C_{22}^{1/2}$ is higher in cellular pads than in honeycombs.

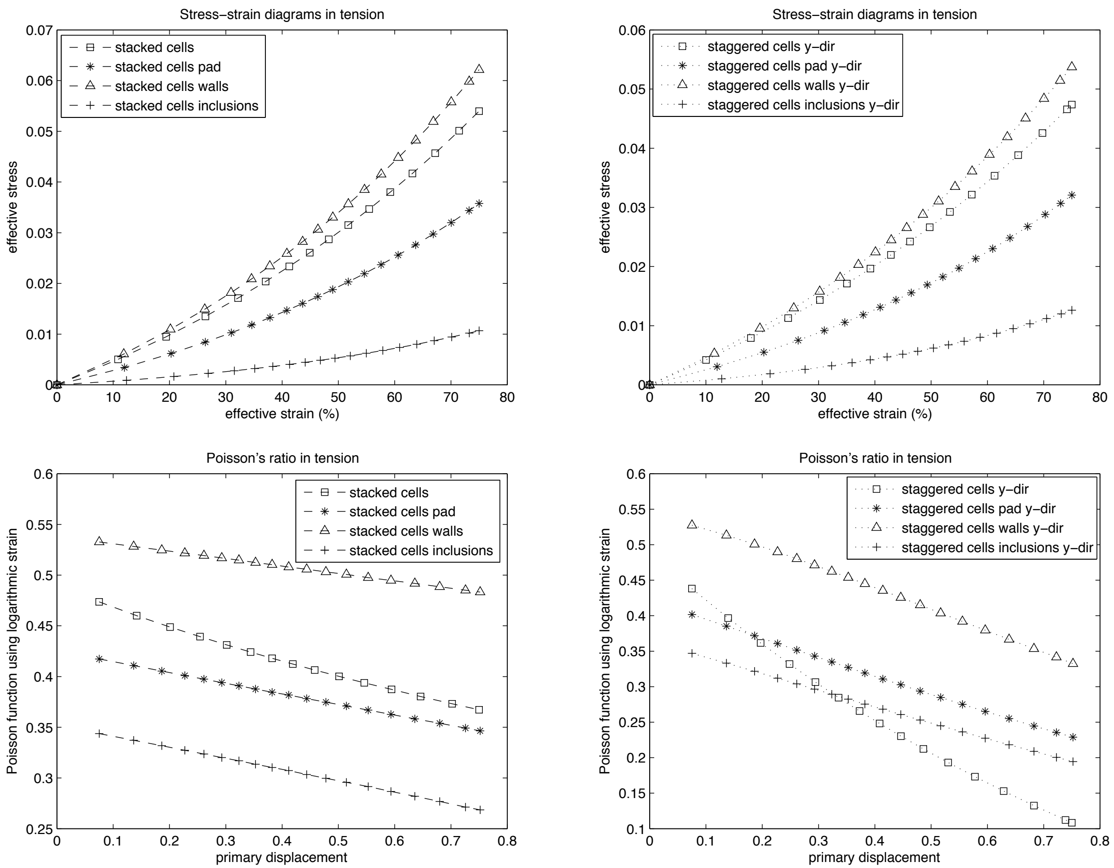

◇ The apparent Poisson's ratio $\nu_L = -\ln C_{11}^{1/2} / \ln C_{22}^{1/2}$ decreases as the vertical tension increases.

Mechanical Behaviour in Vertical Compression

◇ The apparent elastic modulus of cell walls $E_L = \sigma_{22}/\ln C_{22}^{1/2}$ is higher in cellular pads than in honeycombs.

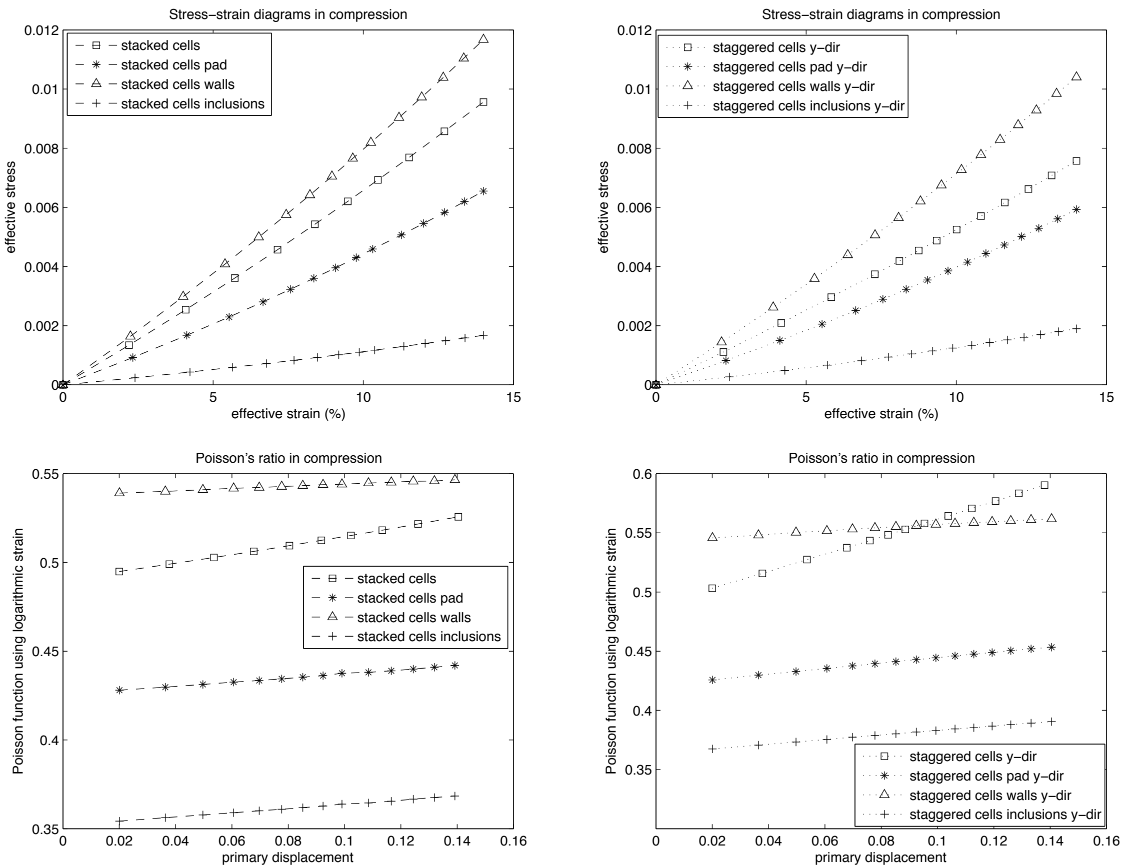

◇ The apparent Poisson's ratio $\nu_L = -\ln C_{11}^{1/2}/\ln C_{22}^{1/2}$ increases as the vertical compression increases.

Combined Tension and Shear

T4. For a horizontal cell wall under combined tension and shear:

$$x = \lambda_1 X, \quad y = K\lambda_1 X + \lambda_2 Y, \quad z = \lambda_3 Z,$$

where $\lambda_{1,2,3} > 0$ independent of $K > 0$, and $\lambda_2 > 1$:

- The apparent elastic modulus:

$$E_L = \frac{\sigma_{22}}{\ln C_{22}^{1/2}} = \frac{-p + \beta_1 \left(e^{-\nu_L \ln \lambda_2^2} - \lambda_1^2 + \lambda_2^2\right) + \beta_{-1}/\lambda_2^2}{\ln \lambda_2}$$

  ◇ is greater in a filled cell than in an empty cell;
  ◇ increases as the thickness of the cell wall increases;
  ◇ increases as the shear increases if $\beta_1 > 0$, $\beta_{-1} \leq 0$ are constants;
  ◇ increases as ν_L decreases if $\beta_1 > 0$, $\beta_{-1} \leq 0$ are constants.

- The apparent Poisson's ratio decreases as the shear increases:

$$\nu_L = -\frac{\ln C_{11}^{1/2}}{\ln C_{22}^{1/2}} = -\frac{\ln \lambda_1^2 (K^2 + 1)}{\ln \lambda_2^2}$$

Combined Compression and Shear

T5. For a horizontal cell wall under combined compression and shear:

$$x = \lambda_1 X, \quad y = K\lambda_1 X + \lambda_2 Y, \quad z = \lambda_3 Z,$$

where $\lambda_{1,2,3} > 0$ independent of $K > 0$, and $\lambda_2 < 1$:

- The apparent elastic modulus:

$$E_L = \frac{\sigma_{22}}{\ln C_{22}^{1/2}} = \frac{-p + \beta_1 \left(e^{-\nu_L \ln \lambda_2^2} - \lambda_1^2 + \lambda_2^2 \right) + \beta_{-1}/\lambda_2^2}{\ln \lambda_2}$$

$\diamond$ is greater in a filled cell than in an empty cell;
$\diamond$ increases as the thickness of the cell wall increases;

$\diamond$ decreases as the shear increases if $\beta_1 > 0$, $\beta_{-1} \leq 0$ are constants;
$\diamond$ decreases as ν_L increases if $\beta_1 > 0$, $\beta_{-1} \leq 0$ are constants.

- The apparent Poisson's ratio increases as the shear increases:

$$\nu_L = -\frac{\ln C_{11}^{1/2}}{\ln C_{22}^{1/2}} = -\frac{\ln \lambda_1^2 (K^2 + 1)}{\ln \lambda_2^2}$$

Honeycombs with Different Cell Geometries in Vertical Tension or Compression

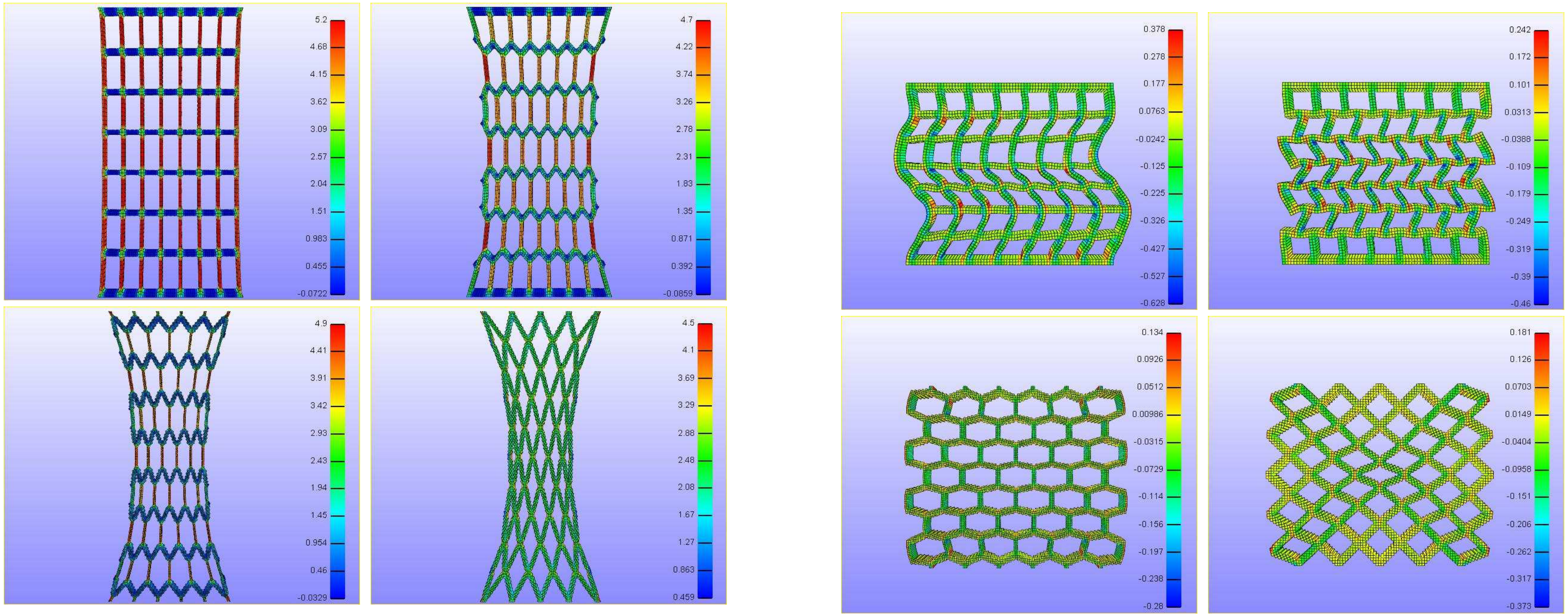

Vertical component of the Cauchy (true) stress tensor σ_{22} under prescribed vertical displacement of 1 (left) and -0.12 (right) at the top boundary [FEBio 2012].

Mechanical Behaviour in Vertical Tension or Compression

◇ In tension, the hexagonal cells are the most flexible, followed by the diamond cells.

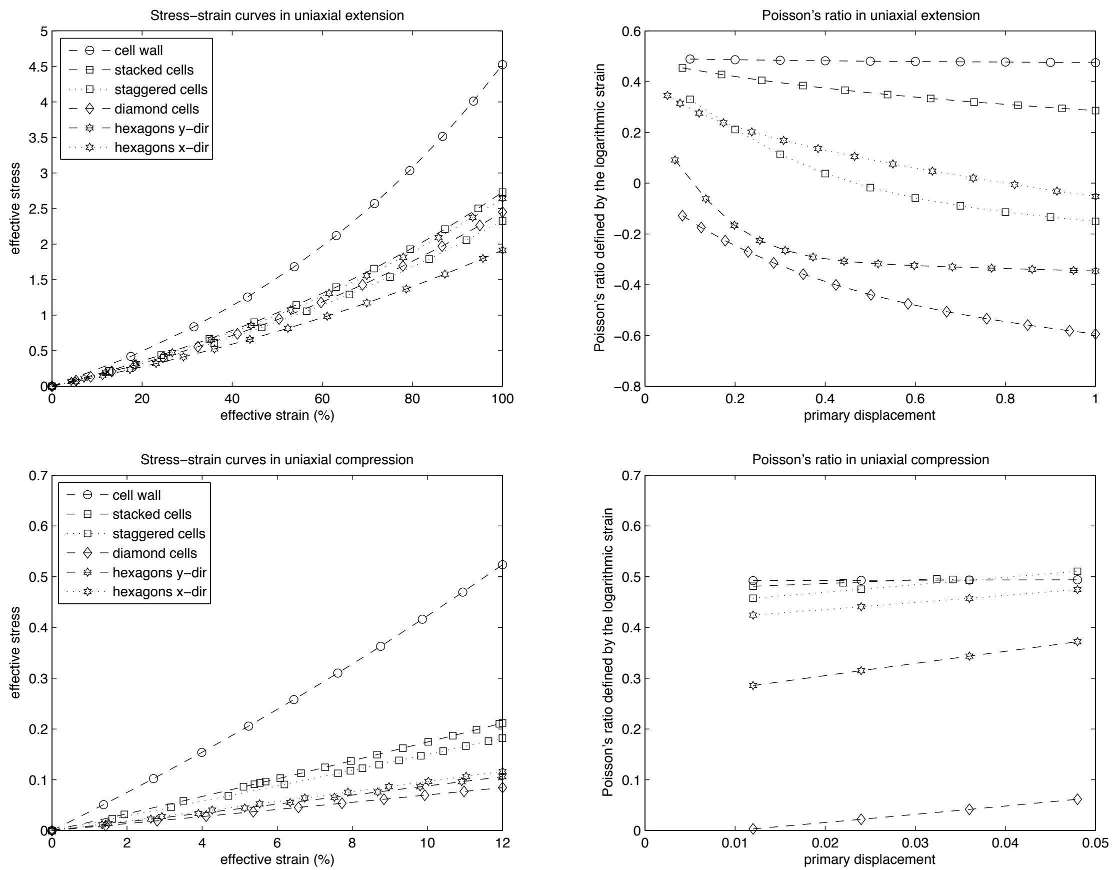

◇ In compression, the diamond cells are the most flexible, followed by the hexagonal cells.

Influence of Oblique Cell Walls

T6. For a cell wall inclined by an angle $\Psi \in (0, \pi/2)$ from the horizontal and subject to vertical shear, the apparent Poisson's ratio $\nu_L = -\ln C_{11}^{1/2} / \ln C_{22}^{1/2}$ decreases as Ψ increases.

- Consider the successive decomposition procedure (SDP):

$$F = \frac{d\boldsymbol{\chi}(X)}{dX}, \quad F' = \frac{d\boldsymbol{\chi}'(X)}{dX}, \quad F'' = \frac{d\boldsymbol{\chi}''(x')}{dx'}$$

  where $\det F' > 0$, $\det F'' > 0$, and $F' = cst$. Then $F = F''F'$.

- The SDP is formally the same as in the constitutive theories of thermoelasticity, elastoplasticity, and growth kinematics.

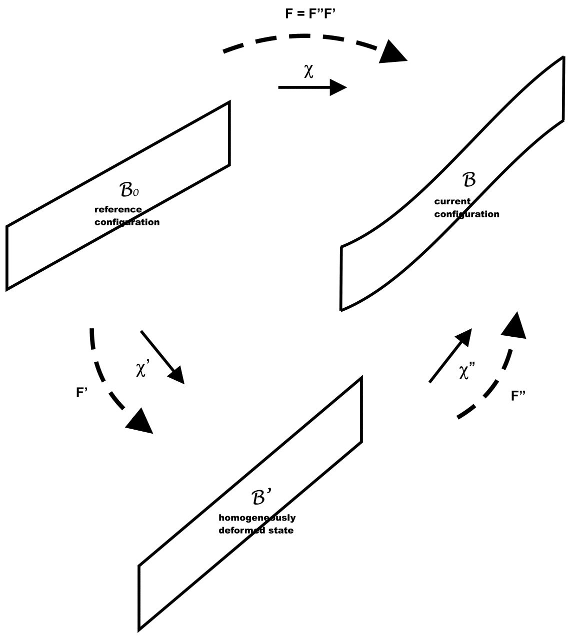

Quantitative Challenges

- For the computational models, rigorous bounds on quantities of physical interest are needed!

$$E_c(F) \leq E_c(F^*) = E_p(u_*) \leq E_p(u)$$

$u \in \mathcal{K}$, $F \in \mathcal{S}$

$$E_p(u) = \int_\Omega \mathcal{W}(F(u))dV - \int_{\Gamma_N} g_N \cdot ud.$$

$$E_c(F) = \int_{\Gamma_D} \frac{\partial \mathcal{W}}{\partial F} u_D \cdot N dA - \int_\Omega \mathcal{W}_c(F$$

◇ [Lee & Shield 1980] (finite elasticity)
◇ [AM & Ainsworth 2009] (linear elastic block structures)
◇ [Livesley 1978] (pioneered the use of linear mathematical programs for rigid block structures)

- Different constitutive materials may behave differently in tension or compression, and hence when subject to more general loading conditions!

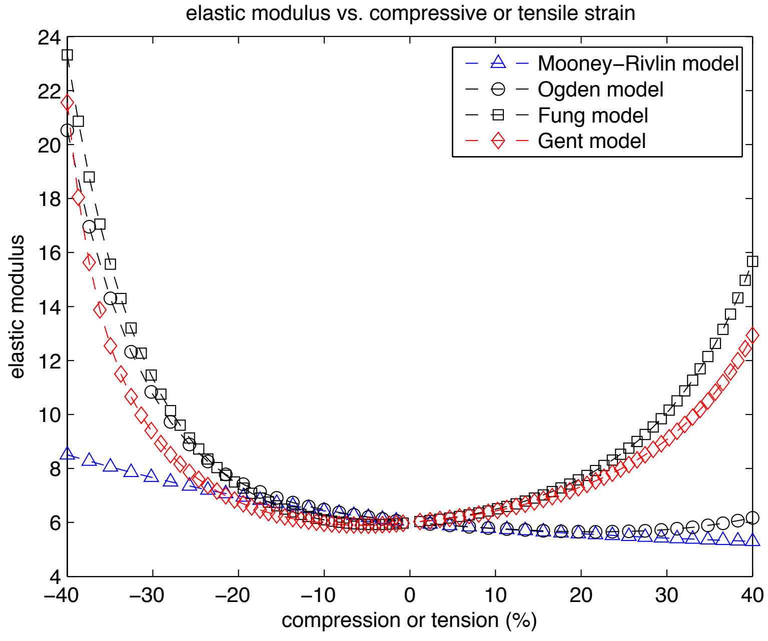

Acknowledgements

Prof. Alain Goriely (Mathematical Modelling, Oxford)

PhD student Khulud Alayyash (Applied Mathematics, Cardiff)

Experiments and computations will be carried out together with
Prof. Sam Evans (Materials, Cardiff) and PDRA during EPSRC project 2015-2017

A 3.5 years research studentship at Cardiff Mathematics is available for a PhD study in the

——————————————————————————————-

‘Elastic Analysis of Biogenic Cellular Structures’ starting in October 2015